Cortical interneurons become activated by deafferentation and instruct the apoptosis of pyramidal neurons

V. E. Koliatsos*†‡§¶, T. M. Dawson†‡‖, A. Kecojevic*, Yueping Zhou*, Yi-Feei Wang*, and K.-X. Huang*

*Department of Pathology, Division of Neuropathology, Departments of †Neurology, ‡Neuroscience, and §Psychiatry and Behavioral Sciences, and ‖Institute for Cell Engineering, The Johns Hopkins Medical Institutions, Baltimore, MD 21205

Edited by Solomon H. Snyder, The Johns Hopkins University School of Medicine, Baltimore, MD, and approved August 19, 2004 (received for review June 18, 2004)

Unlike peripheral nervous system neurons and certain groups of nerve cells in the CNS, cortical projection neurons are tolerant of axonal lesions. This resistance is incongruent with the massive death of pyramidal neurons in age-associated neurodegenerative diseases that proceed along corticocortical connections. Some insights have emerged from our previous work showing that pyramidal cells in piriform cortex undergo classical apoptosis within 24 h after bulbectomy via transsynaptic, but not retrograde, signaling. These findings allow the investigation of cellular and molecular changes that take place in the context of experimental cortical degeneration. In the present study, we show that the transsynaptic death of pyramidal neurons in piriform cortex is a nitric oxide-mediated event signaled by activated interneurons in layer I. Thus, we demonstrate that cortical interneurons play an essential role in transducing injury to apoptotic signaling that selectively targets pyramidal neurons. We propose that this mechanism may be generic to cortical degenerations and amenable to therapeutic interventions.

Studies of neuronal injury and death in the peripheral nervous system (PNS) have been greatly facilitated with the use of simple lesion models, i.e., axotomy, after which motor, sensory, and sympathetic neurons undergo stereotypical retrograde alterations, sometimes progressing to cell death (1, 2). The vulnerability of PNS neurons to axotomy is presumably related to the deprivation of target-derived trophic signals (3–6). In the CNS, the vulnerability of projection neurons to separation from targets is variable. Cortical neurons in particular are viewed as tolerant of axonal lesions (2). This tolerance to injury is puzzling in view of the massive death of cortical pyramidal cells in age-associated neurodegenerative diseases, a phenomenon that appears to follow patterns of corticocortical connectivity (7, 8). Our previous efforts to comprehend the surprising tolerance of cortical neurons to experimental lesions led to the characterization of an experimental model of cortical degeneration in which pyramidal neurons in piriform cortex are vulnerable to ablations of the olfactory bulb (9). In this setting, pyramidal cells undergo classical apoptosis within 24 h after bulbectomy via transsynaptic, but not retrograde, signaling. The lesion effect is powerful, but specific to relay pyramidal neurons located superficially in layer II, in a pattern contrasting the nonselective death of cortical neurons in classical anoxic–ischemic injury. These findings allow the investigation of molecular and cellular changes that take place in the context of transsynaptic cell death, a mechanism speculated to underlie cell death in neurodegenerative disorders involving the cerebral cortex, such as Alzheimer's disease (7, 10, 11).

In the present study, we use anatomical, pharmacological, and molecular methodologies, including genetically altered ($nNOS^{-/-}$) mice, to show that the transsynaptic death of pyramidal neurons in piriform cortex is a nitric oxide (NO)-mediated event initiated by activated interneurons, including reactivated Cajal–Retzius cells. This indirect triggering of apoptosis may serve to target cell death signaling selectively to denervated neurons. The efficiency as well as selectivity of this mechanism suggests its broader role in determining a stepwise elimination of cortical relay neurons in neurological injury and age-associated cortical degenerations.

Materials and Methods

Surgical Lesions to Remove Bulb Afferents to Piriform Cortex in Rats and Mice: Bulbotomies and Bulbectomies. To deprive the piriform cortex of afferents from the olfactory bulb while minimizing the direct impact of the lesion, in rats, we modified the original procedure that involved aspiration bulbectomy (9) and performed needle transections of the olfactory peduncle through a craniotomy window centered 1 mm lateral to frontal suture (bulbotomies). In the mouse, a portion of the primary olfactory bulb is located underneath the frontal pole and, in many cases, immediately adjacent to the rostral piriform cortex; in addition, the olfactory peduncle is situated immediately dorsal to the carotid siphon, and needle manipulations often cause strokes in the territory of the middle cerebral artery. For these reasons, mice were subjected to unilateral aspiration lesions of the bulb after wide paramesial craniotomy at the level of the frontal suture.

Histochemistry and Immunocytochemistry (ICC) for Markers of Normal and Injured/Apoptotic Piriform Cortical Neurons. For histochemical and ICC studies, rats (Sprague–Dawley, male, 250–300 g) were killed at 6, 8, 10, 14, and 20 h after bulbotomy with 3% neutral-buffered paraformaldehyde, and brain blocks containing the entire forebrain were obtained as described (12). In exception to this rule, tissues intended for citrulline ICC were derived from animals perfused with 5% glutaraldehyde/0.5% paraformaldehyde (13). Antibodies and procedures are detailed in *Supporting Text*, which is published as supporting information on the PNAS web site. NADPH diaphorase (NADPHd) histochemistry was performed according to Vincent *et al.* (14). Reelin ICC used the well characterized monoclonal antibody CR-50 (a gift from Kazunori Nakajima, Jikei University, Tokyo). Citrulline ICC used a rabbit antiserum (courtesy of Solomon H. Snyder, The Johns Hopkins Medical School). To study the direct innervation of layer I interneurons by olfactory bulb afferents, we injected the anterograde tracer biotin dextran amine in the olfactory bulb of normal rats. Surgical and histological procedures for the visualization of olfactory bulb terminals in piriform cortex are described in *Supporting Text*.

This paper was submitted directly (Track II) to the PNAS office.

Abbreviations: ICC, immunocytochemistry; NADPHd, NADPH diaphorase; ISH, *in situ* hybridization; NOS, nitric oxide synthase; nNOS, neuronal NOS; 3BR-7NI, 3-bromo-7-nitroindazole; TUNEL, terminal deoxynucleotidyltransferase-mediated dUTP nick end labeling; PARP, poly(ADP-ribose) polymerase.

¶To whom correspondence should be addressed. E-mail: koliat@jhmi.edu.

***In Situ* Hybridization (ISH) for Immediate Early Gene Induction in Piriform Cortex After Bulbotomy.** RNA sense and antisense probes for c-fos and c-jun were prepared essentially as described (15) and detailed in *Supporting Text*. ISH used freshly frozen coronal sections through the piriform cortex of bulbotomized rats killed at 6, 8, 10, 14, and 20 h after lesion and was performed as per standard protocols in our laboratory (15).

Conventional Histology/Cell Counts on Lesioned WT and nNOS$^{-/-}$ Mice. Mice (8 WT, 11 nNOS$^{-/-}$) generated as described (16) were subjected to unilateral bulbectomy. Twenty-four hours after the lesion, animals were killed with neutral-buffered 4% paraformaldehyde. Brain tissues were prepared for stereological counts of normal and apoptotic neurons in piriform cortex by using the optical fractionator probe (17) as detailed in *Supporting Text*.

Pharmacological Inhibition of Neuronal NO Synthase (nNOS). Rats (Sprague–Dawley, male, 250–300 g) were subjected to unilateral bulbotomy or sham operation and treated with the specific nNOS inhibitor 3-bromo-7-nitroindazole (3BR-7NI) (A. G. Scientific, San Diego) in DMSO in two doses given i.p. at the time of lesion and 6 h after surgery. Subjects were divided into five groups, i.e., sham, vehicle, and three dose regimens of 3BR-7NI (60, 20, and 10 mg/kg, $n = 5$ in each group). Animals were killed with neutral-buffered 4% paraformaldehyde 24 h after bulbotomy, and tissues were prepared for stereological counts of apoptotic cells in layer II of olfactory cortex as described in *Supporting Text*.

Stereological Assessment of nNOS/NADPHd(+) Fibers in Layer I of Deafferented Piriform Cortex. NADPHd-stained, systematically selected serial sections through the anterior piriform cortex of bulbotomized or sham-operated rats killed at 8, 14, and 20 h after lesion were analyzed for the areal fraction of nitrinergic fibers in layer I (18) as detailed in *Supporting Text*.

Characterization of Apoptosis in Piriform Cortex: Terminal Deoxynucleotidyltransferase-Mediated dUTP Nick End Labeling (TUNEL) and DNA Gels. TUNEL was performed essentially as described (19) on dry premounted sections from bulbotomized or sham-operated rats 6, 8, 10, 14, and 20 h after lesion. For electrophoresis, DNA was extracted from fresh samples of layer II of piriform cortex at 6, 10, 16, and 22 h after bulbotomy, ^{33}P-end-labeled, and electrophoresed as described (19).

RT-PCR and Real-Time Quantitative RT-PCR for nNOS mRNA. RT-PCR served as a semiquantitative screen for levels of nNOS expression in layer I of piriform cortex 6, 12, 18, and 24 h after bulbotomy or sham surgery. Detailed procedures including primer sequences are described in *Supporting Text*. Based on the results of screening that suggested an increase in nNOS expression 12 h after bulbotomy, we targeted real-time quantitative RT-PCR analysis of nNOS mRNA to that time point by using iQ SYBR Green Supermix (Bio-Rad) (details in *Supporting Text*). The number of PCR cycles (C_t) needed to reach a threshold level of SYBR Green fluorescence corresponding to the linear range of amplification was further normalized by subtracting the C_t for the housekeeping gene GAPDH ($\Delta C_t = C_{t\ \mathrm{nNOS}} - C_{t\ \mathrm{GAPDH}}$). Final outcome was expressed as sham or bulbotomy group difference from the unlesioned group ($\Delta\Delta C_t$).

Western Blotting for Neuronal/Inducible/Endothelial NOS, Poly(ADP-Ribose) Polymerase (PARP), Bax, and Protein Carbonylation. Bulbotomized or sham-operated rats were killed by decapitation 6, 12, 18, or 24 h after lesion, and protein samples from layer I or layer II were separately analyzed for nNOS, inducible NOS, and endothelial NOS (layer I) or PARP and bax (layer II) as described in *Supporting Text*.

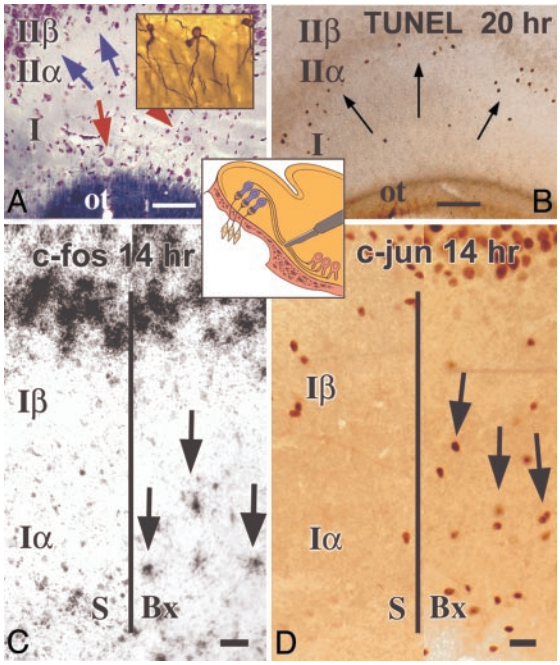

Fig. 1. Disconnection of the olfactory bulb from piriform cortex with bulbotomies causes apoptosis of relay pyramidal neurons located superficially in layer II after early signaling that involves interneurons in outer layer I. (*A* and *B*) Bulbotomies interrupt the innervation of relay neurons in layer IIα (pink pyramidal profiles in *Central Inset*) by mitral cells in the olfactory bulb (blue tufted profiles in *Central Inset*), but do not directly damage the processes of these relay neurons. CV-LFB preparations for cells and fibers and rapid Golgi–Cox silver-stained sections for cell cytology (*A*) show the key cell types involved in the bulbotomy model: pyramidal relay neurons (blue arrows) situated in layer IIα or polymorphic cell layer and interneurons (red arrows) in the outer sector of layer I (Iα or outer plexiform layer); Golgi–Cox preparations (*A Inset*) show the characteristic "semilunar" cytology of relay neurons with their exclusively apical dendrites traversing the plexiform layer. The degenerative impact of bulbotomy is selective to layer IIα neurons, as shown in a TUNEL preparation (*B*) through the intermediate piriform cortex (arrows). (*C* and *D*) Bulbotomy lesions activate neurons in layer Iα 10–14 h after lesion as shown by immediate early gene ICC and ISH. Panels depict c-fos ISH (*C*) and c-jun ICC (*D*) preparations from subjects with sham (S) or bulbotomy (Bx) lesions killed 14 h after surgery. ot, olfactory tract. (Scale bars, 100 μm in *A* and *B* and 20 μm in *C* and *D*.)

Results

Early Signaling in Deafferented Piriform Cortex Is an Event Extrinsic to Degenerating Neurons: The Transsynaptic Activation of nNOS-Expressing Interneurons of Layer I. Ablations of the olfactory bulb cause transsynaptic death of 53,400 neurons in layer IIα of the corresponding idiotypic sensory (piriform) cortex (9). To confirm that bulbotomies have the same transsynaptic effect, we studied TUNEL-stained sections 6, 8, 10, 14, and 20 h after lesion. Staining of condensed/fragmented nuclei appeared in layer IIα by 14 h and became intense at 20 h; these results validate that bulbotomy lesions used in this study are indistinguishable from bulbectomies in causing transsynaptic apoptosis of semilunar pyramids of layer IIα (Fig. 1 *A* and *B*).

Immediate early gene (c-fos and c-jun) ICC and ISH were used to screen for cellular activation in piriform cortex before the apoptotic peak, i.e., 6–20 h after bulbotomy. Remarkably, little or no change was seen in layer IIα. The greatest activation was observed in interneurons and astrocytes in the external half of layer I (Iα) and was evident 10–14 h after lesion (Fig. 1 *C* and *D* and

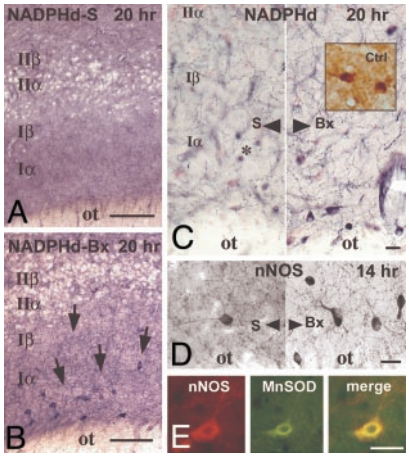

Fig. 2. Layer Iα interneurons activated by bulbotomy express nNOS. Localization of increased levels of nNOS in the cell bodies and, especially, axons of layer Iα interneurons 10–20 h after bulbotomy by NADPHd histochemistry (*A–C*) and nNOS ICC (*D*). (*A* and *B*) Low-magnification images show the specificity of nNOS/NADPHd staining for the cell bodies and processes of layer I neurons, especially after bulbotomy (Bx, arrows); no NADPHd(+) neurons are visible in layer II. (*C* and *D*) *Left* and *Right* contrast the sham (S) with the bulbotomy (Bx) condition. Layer Iα interneurons also stain with citrulline antibodies (*C Right Inset*) 14–20 h after lesion on specially prepared tissues. Several ring-like NADPHd(+) structures (examples are indicated by asterisk in *C*) belong to cross-sections of blood vessels and do not stain with nNOS antibodies (*D*). (*E*) Besides nNOS, manganese superoxide dismutase (MnSOD) expression is also induced in layer Iα interneurons after bulbotomy, as shown in immunofluorescent preparations dually stained for nNOS and MnSOD. Bx, bulbotomy; Ctrl, citrulline; ot, olfactory tract; S, sham. (Scale bars, 100 μm in *A* and *B* and 20 μm in *C–E*.)

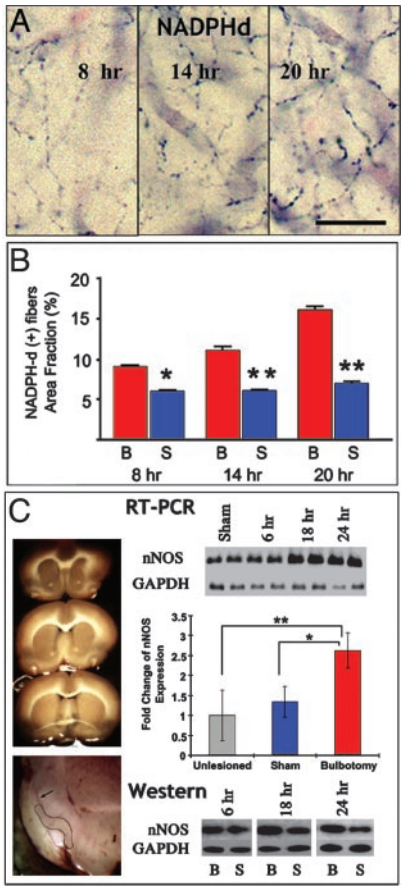

Fig. 3. NOS expression is up-regulated in layer Iα interneurons after bulbotomy, as shown by histochemical (*A* and *B*) and biochemical (*C*) analyses. (*A* and *B*) By NADPHd histochemistry, a large portion of nNOS is localized to axonal branches of layer I interneurons that ramify throughout layer I. Density of histochemically reactive layer I fibers increases progressively 8–20 h after bulbotomy, and differences between sham and bulbotomized animals are significant throughout this time period by ANOVA followed by post hoc testing (*B*). Overall, $P < 0.0001$; post hoc: *, $P < 0.01$ and **, $P < 0.001$. (*C*) Biochemical studies of nNOS expression in microdissected samples of layer I from three anteroposterior planes of piriform cortex indicated in *Upper Left*. Layer-specific dissection was aided by staining of fresh slices with nonalcoholic hematoxylin (*Lower Left*; dissected area is delineated by solid line; layer II staining is indicated with an arrow). By semiquantitative RT-PCR screening (*Top Right*; each condition represented by two lanes), standardized nNOS mRNA (nNOS/GAPDH) was found to be increased, compared to sham, at 12–24 h after bulbotomy; the difference at 18 and 24 h was significant at $P < 0.005$. Real-time RT-PCR confirmed the up-regulation of nNOS mRNA 12 h after lesion (*Middle Right*). Bars represent standardized ($\Delta\Delta C_t$) changes against GAPDH expression in unlesioned piriform cortex (gray column set as 1) and are significant between bulbotomized and sham animals (by *t* test, $P < 0.05$). By Western blotting, nNOS protein is also found increased 12–24 h after lesion (*Bottom Right*); each condition is represented here by a single lane, sham (S) juxtaposed to bulbotomy (B) for each time point. (Scale bar in *A*, 20 μm.)

Fig. 8, which is published as supporting information on the PNAS web site). Dual-label ICC for c-fos and 2′,3′-cyclic nucleotide 3′-phosphodiesterase or c-fos and myelin basic protein (MBP) (for immature and mature oligodendrocytes, respectively) or c-fos and the microglial marker OX-42 (for microglia) did not produce double-labeled profiles up to 14 h after bulbotomy.

Consistent with the activation of layer Iα, NADPHd histochemistry/nNOS ICC revealed a population of interneurons in proximity to the lateral olfactory tract, evident only in bulbotomized animals (Fig. 2 *A–D*). These layer-Iα interneurons become apparent 10 h after lesion and continue to be highly reactive for NADPHd/nNOS at 20 h. The presence of citrulline immunoreactivity in these neurons 14 and 20 h after lesion (Fig. 2*C Inset*) indicates that nNOS induction is associated with the release of NO. The absence of TUNEL staining in layer Iα up to 48 h after lesion indicates that bulbotomy does not cause the degeneration of layer Iα interneurons. At least part of the cause for the persistence of these cells may be the expression of manganese superoxide dismutase (MnSOD) evident at 14 and 20 h after lesion, but not at earlier time points or in sham-operated animals (Fig. 2*E*) (20, 21).

Most NADPHd/nNOS reactivity in piriform cortex is localized in the axons of layer Iα interneurons that branch extensively throughout layer I (Figs. 2 *C* and *D* and 3*A*). Stereological counts of these axons show an increase at 8 h after lesion with a further significant increment at 20 h (Fig. 3*B*). The rapidity of this response indicates nNOS overexpression, rather than *de novo* axonal branching. This prediction is consistent with increased perikaryal nNOS staining in layer I and is confirmed with nNOS expression screening by semiquantitative RT-PCR or Western blotting at different time points after lesion. By both analyses, nNOS mRNA and protein progressively increased in layer I beginning at 12 h after bulbotomy. By real-time RT-PCR, nNOS mRNA increased 2.5-fold compared to unlesioned piriform cortex at 12 h; this difference is significant when we consider the lack of change in sham-operated animals (Fig. 3*C*). No changes were found in the expression of inducible and endothelial NOS by Western screening up to 20 h after lesion.

nNOS Gene Deletion or Pharmacological Inhibition Rescues Neurons in Piriform Cortex from Transsynaptic Degeneration. To assess the significance of nNOS up-regulation for the apoptotic outcome of bulbotomy, we examined the effect of suppressing nNOS activity by gene ablation or pharmacological inhibition of the enzyme on numbers of dying neurons. $nNOS^{-/-}$ and WT mice were sub-

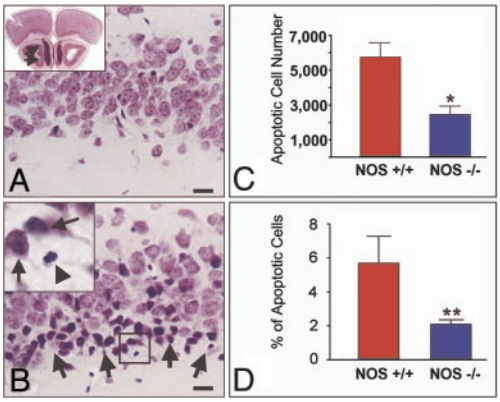

Fig. 4. Confirmation of the significance of nNOS/NO signaling for transsynaptic apoptosis in piriform cortex with bulb lesions in $nNOS^{-/-}$ mice. (*A Inset*) A comment on the anatomy of the mouse olfactory bulb. (*B Inset*) A magnification of the framed area in *B*. (*A* and *B*) In WT mice, bulb lesions cause transsynaptic degeneration of layer IIα neurons 24 h after lesion. Compare a sham-operated (*A*) with a bulbectomized (*B*) animal. Degenerating neurons (*B*) show shrinkage and pyknosis (arrows in *Inset*); fragmentation of the nucleus is also evident in some cells (arrowhead in *Inset*). As shown in *A Inset*, a substantial portion of the mouse olfactory bulb is located underneath the frontal pole (arrows); this anatomical feature makes it necessary to employ careful aspiration lesions, as explained in *Materials and Methods*. (*C* and *D*) In $NOS^{-/-}$ mice, piriform neurons undergoing transsynaptic degeneration after bulbectomy are significantly reduced in both number (*C*) and percentage in the total number of layer I-II pyramidal neurons. (*D*). *, $P = 0.0167$; **, $P = 0.0015$. (Scale bars, 20 μm.)

jected to aspiration bulbectomies (Fig. 4*A*), and numbers of total neurons in layers I–II of anterior piriform cortex as well as numbers of apoptotic profiles were counted with stereological methods (Fig. 4 *A* and *B*). Twenty-four hours after bulbectomy, we detected ≈6,000 apoptotic profiles (corresponding to ≈6% of layer I–II neurons) in the piriform cortex of WT animals; in nNOS-null mice, we counted ≈2,500 apoptotic profiles (corresponding to ≈2% of layer I–II neurons), i.e., a significant reduction by 3,500 profiles when compared to WT littermates (Fig. 4 *C* and *D*). Inhibition of nNOS activity by the nNOS-specific compound 3BR-7NI in doses that result in near total blockade of the enzyme in the brain (Fig. 5 *Upper*) ameliorated transsynaptic apoptosis in piriform cortex. Doses in the range of 20–60 mg/kg were particularly effective (Fig. 5 *Lower*).

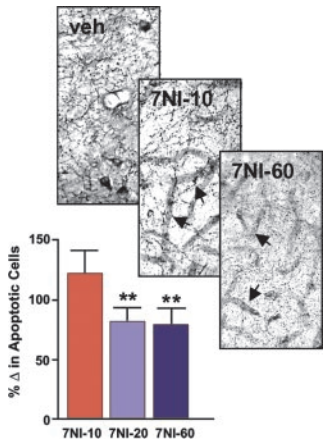

Fig. 5. Pharmacological blockade of nNOS with the selective inhibitor 3BR-7NI ameliorates transsynaptic apoptosis in piriform cortex. Although 10 mg/kg appeared to inhibit nNOS/NADPHd activity within individual neurons (*Upper*; compare veh with 7NI-10), it was with 20 and 60 mg/kg of 3BR-7NI that the enzyme was also blocked within neuronal processes (*Upper*, 7NI-60). Consistent with the specificity of 3BR-7NI for nNOS, no significant inhibition was seen in NADPH activity seen in conjunction with blood vessels (*Upper*, arrows in 7NI-10 and 7NI-60). (*Lower*) Corresponding to the NADPHd blockade data, doses of 3BR-7NI at 20 and 60, but not 10, mg/kg caused statistically significant decreases in apoptotic profiles counted 24 h after bulbotomy. Bars represent percentile differences from vehicle (veh) group. ANOVA, $P = 0.0015$, attributable to $P < 0.01$ difference between 7NI-20 or 7NI-60 from the 7NI-10 group.

nNOS Induction in Deafferented Piriform Cortex Is Associated with Downstream Signaling Consistent with NO-Mediated Cell Death. To confirm the suggestion that NO is a critical upstream signal for the activation of apoptosis in layer II neurons, we processed microdissected samples of layer II for DNA fragmentation, markers of oxidative-free radical injury, and the expression/processing of proteins known to execute downstream steps in NO-mediated cell death (Fig. 6). DNA electrophoresis showed some oligonucleosomal fragmentation at 16 h and was robust by 22 h (Fig. 6*A*). Protein oxidative damage as shown by excessive carbonylation was an earlier event, beginning at 10 h and becoming intense by 12 h (Fig. 6*B*). At 12 h after bulbotomy (i.e., a time point coinciding with increased nNOS expression in layer I), Western blotting showed PARP cleavage to p85 and up-regulation of bax (Fig. 6*C*). The latter was confirmed with ICC 14 and 20 h after bulbotomy (Fig. 6*D*). At 20 h, many neurons in layer IIα also stained with antibodies specific for active caspase 3 (Fig. 6*E*). These observations divulge key events critical for the mediation of NO-induced cell death, i.e., downstream oxidative injury including DNA damage to vulnerable neurons and further downstream cytosolic activation of proteins of the caspase and bcl-2 family. These events occur at times compatible with their role in the apoptosis of layer II neurons.

Layer I Piriform Neurons Activated by Bulb Lesions Are Reelin(+) Interneurons. The implication of interneurons in the initial signaling of transsynaptic apoptosis of pyramidal neurons in piriform cortex raises further questions about the identity of these cells and their role in the regulation of cortical cell number. nNOS expression in layer I is developmentally related to Cajal–Retzius cells, the first postmitotic neurons of cerebral cortex that die or become dormant after the completion of cortical development (22, 23). To explore the hypothesis that Cajal–Retzius or phenotypically related cells become reactivated after lesions of the mature piriform cortex, we stained sections through the piriform cortex of lesioned or sham animals with the monoclonal antibody CR-50 directed against the glycoprotein reelin, a specific marker of Cajal–Retzius cells (24). In normal animals, many CR-50(+) cells were seen in the outer portions of piriform cortex embedded in a reelin-rich neuropil that precisely delineated layer Iα (Fig. 7*A*). Based on dual ICC for c-fos and CR-50, reelin(+) neurons are activated 10–14 h after bulbotomy, i.e., coinciding with the general induction of cells in layer Iα after bulb lesions (Fig. 9, which is published as supporting information on the PNAS web site). Dual-label ICC for CR-50 and nNOS showed that, 10–14 h after bulbotomy, almost all reelin(+) cells in layer I are also reactive for nNOS (Fig. 7 *B–D*). At least half of neurons dually labeled for CR-50 and nNOS have the cytological features of Cajal–Retzius cells (Fig. 7 *B–D*). Besides reelin, Cajal–Retzius cells express calcium binding proteins and γ-aminobutyric acidergic neurotransmitter markers in various degrees and stages of development (22, 25). Dual ICC for nNOS or reelin with calbindin, calretinin, and glutamic acid decarboxylase (GAD) 14 h after bulbotomy reveals a 50% colocalization between nNOS and GAD, but not nNOS/reelin and calbindin or nNOS/reelin and calretinin in layer I neurons (Fig. 10, which is published as supporting information on the PNAS web site).

The early activation of reelin(+) interneurons in the mature piriform cortex after bulbotomy is made possible via their direct

NEUROSCIENCE

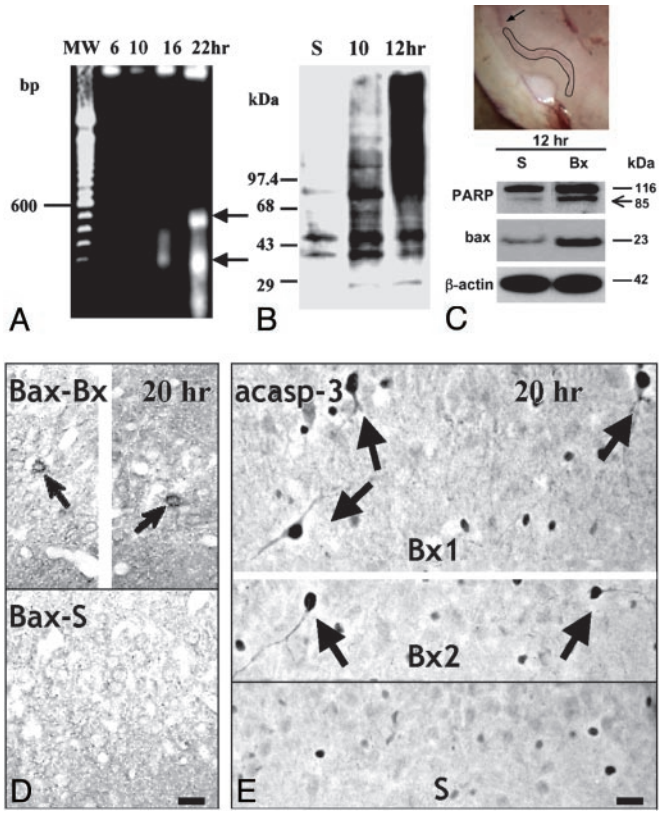

Fig. 6. Evidence of free radical release, DNA injury, and cytosolic signaling of apoptosis on microdissected samples of layer II piriform cortex. (*A Inset*) The layer II-specific dissection, as compared to layer I dissection illustrated in Fig. 3*C*. (*A*) DNA blots show fragmentation in nucleosomal multimers. There are ≈200- and ≈400-bp multinucleosomal bands 22 h after bulbotomy (arrows), but some nonrandom fragmentation is also seen by 16 h. (*B*) Oxyblot detection of extensive carbonylation of proteins in layer II of piriform cortex 10–12 h after bulbotomy. (*C*) Twelve hours after bulbotomy, i.e., at a time point overlapping with oxidative injury as in *B* and upstream to DNA fragmentation (*A*), Western blotting shows evidence of DNA injury based on PARP cleavage and cytosolic signaling of apoptosis based on bax up-regulation. (*Upper*) The layer-II specific dissection that generated samples for analyses in *A–C*; compare with layer I dissection illustrated in Fig. 3*C*. (*D*) At 14–20 h after bulbotomy, bax protein accumulates in layer II neurons (arrows) at levels detectable by ICC. (*Upper*) Because of space limitations, the image was edited by removing the middle and approximating the medial and lateral portions of the section. (*E*) Twenty hours after bulbotomy, several layer IIα profiles developed strong immunoreactivity to active caspase 3 (arrows). (*Upper*) Two bulbotomy cases. (*Lower*) The sham condition. Specific immunoreactivity is localized to the cytoplasm. Some nonspecific nuclear staining is present in many cells both in the bulbotomy and sham scenarios. Bx, bulbotomy; S, sham. (Scale bar, 20 μm.)

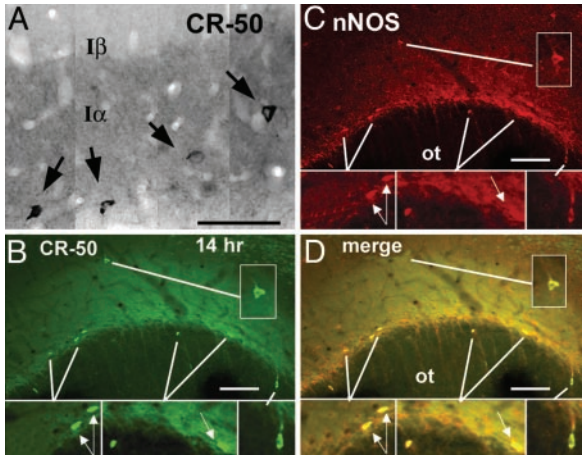

Fig. 7. Identification of bulbotomy-induced interneurons in piriform cortex as reelin(+) neurons based on CR-50 (*A*) and colocalization of CR-50 with nNOS (*B–D*). (*A*) ICC for reelin with the well characterized antibody CR-50 identifies highly immunoreactive small-to-medium size neurons (arrows) embedded in a reelin-rich neuropil that overlaps precisely the borders of layer Iα. (*B–D*) Dual immunofluorescence for reelin and nNOS shows increased nNOS immunoreactivity in seven CR-50 (+) neurons in layer I 14 h after bulbotomy. Bipolar perikarya with their long axis parallel to the border with the olfactory tract are identical to Cajal–Retzius cells (arrows). (*Insets*) Magnifications of demarcated areas. ot, olfactory tract. (Scale bars, 100 μm.)

innervation from mitral cell axons that are transected with this lesion. In anterograde labeling experiments using the axonal marker biotin dextran amine combined with CR-50 ICC, we found synaptic boutons from mitral cell axons apposed to the cell bodies of reelin(+) neurons in confocal microscopic analysis followed by three-dimensional reconstruction (Fig. 11, which is published as supporting information on the PNAS web site).

Discussion

Taken together, the findings of this study indicate that transsynaptic apoptosis of pyramidal neurons in piriform cortex is signaled by inducible inhibitory interneurons. First, we have shown the induction of nNOS expression in a subset of layer I interneurons 6–8 h before the apoptotic death of pyramidal neurons. Second, we have shown that nNOS gene deletion or pharmacological inhibition rescues a substantial number of pyramidal neurons from transsynaptic degeneration, a pattern suggesting that NO released by layer I interneurons is a critical upstream signal for the initiation of apoptosis. This contention is consistent with the absence of early activation, after bulbotomy, of other cells known to initiate or mediate neuronal cell death, such as phagocytic microglia (9) and the generally accepted role of NO in signaling neuronal apoptosis (26, 27). The role of NO as an apoptotic signal in the bulbotomy model is further supported by our molecular studies on microdissected samples of layer II that reveal cellular and molecular events consistent with the downstream execution of NO-mediated cell death. Third, we have generated some insights into the identity of layer I interneurons implicated in the triggering of transsynaptic apoptosis. These nerve cells express phenotypic markers (e.g., reelin and GAD) and have the cytological features of inhibitory cortical interneurons, possibly including dormant Cajal–Retzius cells. The direct recipients of olfactory bulb axons, these interneurons are induced, by anterograde signals related to bulbotomy, to synthesize and release NO via a dense plexus of axonal branches. Volume signaling models of release and passive diffusion of NO predict an idealized circular target area with a 100-μm radius (28, 29), i.e., within reach for neurons located superficially, but not deeply, in layer II. Although the selective degeneration of layer IIα neurons may be the mere effect of proximity to NO-releasing interneurons, we cannot rule out the contribution of signals from degenerating terminals of mitral cell axons apposed directly to the distal dendrites of layer IIα neurons or the deprivation of anterogradely transported trophic factors, e.g., brain-derived neurotrophic factor. Together, these mechanisms may serve to eliminate cortical projection neurons that, for whatever reason, are excluded from functional circuits. The activation of small nNOS(+) interneurons may be implicated in the mediation of cortical apoptosis in models beyond deafferentation, such as *N*-methyl-D-aspartate antagonist-induced apoptosis of pyramidal neurons in piriform cortex and elsewhere.**

Death of cortical neurons by transsynaptic apoptosis and NO-induced necrosis in models of anoxic injury/stroke appear

**Welsh, A. M. & Koliatsos, V. E. (2003) *Soc. Neurosci. Abstr.*, p. 29 (abstr.).

to involve similar downstream cellular steps except that, in the former, levels of superoxide anion may not be as elevated as in the latter (27). This difference may determine the type of cell death, with apoptosis predominating in transsynaptic injury and necrosis prevailing in models of stroke. However, what is qualitatively unique about transsynaptic cortical cell death compared to anoxic/ischemic injury is the delegation of the injurious role to a set of cortical interneurons, rather than a direct effect via *N*-methyl-D-aspartate receptors (26). Certain populations of cortical interneurons may serve to both amplify the transsynaptic effect and target it to a select population of cortical projection neurons. This cellular model accounts for a more controlled, selective death of cortical neurons. However, if the initial injury signals persist, apoptosis may be further propagated in the anterograde fashion via corticocortical connections. This model predicts a higher risk for cortical neurons with reciprocal connections and multiple convergent afferent inputs, i.e., neurons of associative cortices and of entorhinal cortex, as it is encountered in age-associated degenerations of the cerebral cortex.

This work was supported by National Institutes of Health Grant RO1 AG16263.

1. Snider, W. D., Elliott, J. L. & Yan, Q. (1992) *J. Neurobiol.* **23,** 1231–1246.
2. Koliatsos, V. E. & Price, D. L. (1996) *Brain Pathol.* **6,** 447–465.
3. Hamburger, V., Brunso-Bechtold, J. K. & Yip, J. W. (1981) *J. Neurosci.* **1,** 60–71.
4. Johnson, E. M., Jr. (1978) *Brain Res.* **141,** 105–118.
5. Oppenheim, R. W., Maderdrut, J. L. & Wells, D. J. (1982) *J. Comp. Neurol.* **210,** 174–189.
6. Ehlers, M. D., Kaplan, D. R., Price, D. L. & Koliatsos, V. E. (1995) *J. Cell Biol.* **130,** 149–156.
7. Hof, P. R. & Morrison, J. H. (1994) in *Alzheimer Disease*, eds. Terry, R. D., Katzman, R. & Bick, K. L. (Raven, New York), pp. 197–229.
8. Troncoso, J. C., Sukhov, R. R., Kawas, C. H. & Koliatsos, V. E. (1996) *J. Neuropathol. Exp. Neurol.* **55,** 1134–1142.
9. Capurso, S. A., Calhoun, M. E., Sukhov, R. R., Mouton, P. R., Price, D. L. & Koliatsos, V. E. (1997) *J. Neurosci.* **17,** 7372–7384.
10. Braak, H. & Braak, E. (1990) in *Alzheimer's Disease*, eds. Maurer, K., Riederer, P. & Beckmann, H. (Springer, New York), pp. 85–91.
11. Arnold, S. E., Hyman, B. T., Flory, J., Damasio, A. R. & Van Hoesen, G. W. (1991) *Cereb. Cortex* **1,** 103–116.
12. Koliatsos, V. E., Price, D. L., Gouras, G. K., Cayouette, M. H., Burton, L. E. & Winslow, J. W. (1994) *J. Comp. Neurol.* **343,** 247–262.
13. Eliasson, M. J., Huang, Z., Ferrante, R. J., Sasamata, M., Molliver, M. E., Snyder, S. H. & Moskowitz, M. A. (1999) *J. Neurosci.* **19,** 5910–5918.
14. Vincent, S. R., Johansson, O., Hokfelt, T., Skirboll, L., Elde, R. P., Terenius, L., Kimmel, J. & Goldstein, M. (1983) *J. Comp. Neurol.* **217,** 252–263.
15. Koliatsos, V. E., Price, D. L., Clatterbuck, R. E., Markowska, A. L., Olton, D. S. & Wilcox, B. J. (1993) *Ann. N.Y. Acad. Sci.* **695,** 292–299.
16. Huang, P. L., Dawson, T. M., Bredt, D. S., Snyder, S. H. & Fishman, M. C. (1993) *Cell* **75,** 1273–1286.
17. West, M. J., Slomianka, L. & Gundersen, H. J. G. (1991) *Anat. Rec.* **231,** 482–497.
18. Vehmas, A. K., Kawas, C. H., Stewart, W. F. & Troncoso, J. C. (2003) *Neurobiol. Aging* **24,** 321–331.
19. Liu, Z., Gastard, M., Verina, T., Bora, S., Mouton, P. R. & Koliatsos, V. E. (2001) *J. Comp. Neurol.* **441,** 1–8.
20. Keller, J. N., Kindy, M. S., Holtsberg, F. W., St. Clair, D. K., Yen, H. C., Germeyer, A., Steiner, S. M., Bruce-Keller, A. J., Hutchins, J. B. & Mattson, M. P. (1998) *J. Neurosci.* **18,** 687–697.
21. Gonzalez-Zulueta, M., Ensz, L. M., Mukhina, G., Lebovitz, R. M., Zwacka, R. M., Engelhardt, J. F., Oberley, L. W., Dawson, V. L. & Dawson, T. M. (1998) *J. Neurosci.* **18,** 2040–2055.
22. Marin-Padilla, M. (1998) *Trends Neurosci.* **21,** 64–71.
23. Santacana, M., Uttenthal, L. O., Bentura, M. L., Fernandez, A. P., Serrano, J., de Velasco, J. M., Alonso, D., Martinez-Murillo, R. & Rodrigo, J. (1998) *Dev. Brain Res.* **111,** 205–222.
24. Ogawa, M., Miyata, T., Nakajima, K., Yagyu, K., Seike, M., Ikenaka, K., Yamamoto, H. & Mikoshiba, K. (1995) *Neuron* **14,** 899–912.
25. Meyer, G., Goffinet, A. M. & Fairen, A. (1999) *Cereb. Cortex* **9,** 765–775.
26. Lipton, S. A., Choi, Y.-B., Pan, Z.-H., Lei, S. Z., Chen, H.-S. V., Sucher, N. J., Loscalzo, J., Singel, D. J. & Stamler, J. S. (1993) *Nature* **364,** 626–632.
27. Bonfoco, E., Krainc, D., Ankarcrona, M., Nicotera, P. & Lipton, S. A. (1995) *Proc. Natl. Acad. Sci. USA* **92,** 7162–7166.
28. Wood, J. & Garthwaite, J. (1994) *Neuropharmacology* **33,** 1235–1244.
29. Philippides, A., Husbands, P. & O'Shea, M. (2000) *J. Neurosci.* **20,** 1199–1207.